Evaluation of the WRF-Lake Model over Two Major Freshwater Lakes in China

Yuanyuan MA[1,2], Yi YANG[1*], Chongjian QIU[1], and Chenghai WANG[1]

1 *Key Laboratory for Semi-Arid Climate Change of the Ministry of Education*, *College of Atmospheric Sciences*, *Lanzhou University*, *Lanzhou* 730000

2 *Key Laboratory of Land Surface Process and Climate Change in Cold and Arid Regions*, *Northwest Institute of Eco-Environment and Resources*, *Chinese Academy of Sciences*, *Lanzhou* 730000

(Received May 21, 2018; in final form December 14, 2018)

ABSTRACT

This paper evaluates the performance of the Weather Research and Forecasting (WRF) model coupled with a lake scheme over the Lake Poyang and Lake Dongting regions. We choose several cases with different weather characteristics, including winter with/without precipitation and summer with/without precipitation, and conduct a series of experiments (without the lake model, with the default lake model, and with a calibrated lake model that adjusts the water absorption, extinction coefficients, and surface roughness length) for each case. The results show that the performance of the lake model is significantly affected by the weather conditions. For the winter with precipitation cases, the performance of the default lake model is even worse than without the lake model, but the calibrated lake model can obviously reduce the biases of 2-m temperature and dew-point temperature. Although the performance of the default and new calibrated models is intricate for other cases, the new calibrated model has prominent advantages for 2-m dew-point temperature. Moreover, a long-term simulation of five months also shows that the new calibrated coupled lake model performs better than the default one. These imply that the new calibrated coupled lake model is more suitable to be used in studies of the effects of Lake Poyang and Lake Dongting on regional weather and climate.

Key words: atmosphere–lake coupled model, Lake Poyang, Lake Dongting, calibration, weather characteristics

Citation: Ma, Y. Y., Y. Yang, C. J. Qiu, et al., 2019: Evaluation of the WRF-lake model over two major freshwater lakes in China. *J. Meteor. Res.*, **33**(2), 219–235, doi: 10.1007/s13351-019-8070-9.

1. Introduction

Lakes play an irreplaceable role in regulating regional climate and maintaining regional ecosystem balance and biodiversity. Lake–atmosphere interaction is a crucial part of regional water cycles and energy budgets (Notaro et al., 2013), and affects weather and climate at the regional scale (Dutra et al., 2010; Samuelsson et al., 2010) through lake effect precipitation (snow), lake breeze (Sills et al., 2011), and other phenomena. Thus, the effects of these relatively broad and slowly flowing bodies of water on weather and climate have become an interesting issue in atmospheric sciences (Balsamo et al., 2012; Martynov et al., 2016).

China is home to many lakes, e.g., Lake Poyang and Lake Dongting are the two largest freshwater lakes, with areas of 3000 and 2600 km^2, respectively. Compared to the surrounding land, lakes have different albedos, larger heat capacities, and smoother surfaces, meaning that they can modify air masses by exchanging heat and moisture with the atmosphere and thus play an important role in local weather and climate (Scott and Huff, 1996; Schmidlin, 2005; Long et al., 2007). Lake Poyang can add warmth to the atmosphere, enhancing heavy precipitation (Fu, 2013). Lake Dongting induces lake breezes approximately 30 m thick, which could increase morning and evening precipitation (Lin and Li, 1988). Additionally, such large lakes could strengthen tropical cyclones that pass over them, extending their life cycles (Wang and Liu, 2008).

As a model resolution has increased, lakes, especially for large lakes, have become an essential underlying sur-

Supported by the National Nature Science Foundation of China (41330527 and 41675098).

*Corresponding author: yangyi@lzu.edu.cn.

face. Additionally, the importance of lake–atmosphere interaction has been indicated (Gao et al., 2012; Bullock et al., 2014; Mallard et al., 2014, 2015). Lake models, which can provide surface momentum, water, and heat fluxes as boundary conditions for weather or climate models, have been indispensable for studies of lake-effect weather. The Hostetler based the lake model has recently been coupled to the Weather Research and Forecasting (WRF) model. Gu et al. (2014) examined the performance of the atmosphere–lake coupled model for Lake Tai using observations from 11 to 28 August 2010, and found that the lake model improved the lake surface temperature (LST) simulations compared to the WRF model without the lake scheme; however, there were significant LST cold biases. Subsequently, Gu et al. (2015) demonstrated the coupled model's performance in the Great Lakes region and showed that the lake model simulated LST well for Lake Erie, but generated strong LST biases (up to ± 20°C) for Lake Superior. Xu et al. (2016) evaluated the lake model for Lake Erhai and found that it presented significant LST bias with default parameters. Coincidentally, these studies all successfully reduced LST biases by calibrating the fraction of solar radiation absorbed by lake water, surface roughness length, and light extinction coefficient.

Moreover, the impacts of lakes on regional weather and climate vary depending on location and season (Notaro et al., 2013; Klaić and Kvakić, 2014). In general, unfrozen lakes tend to suppress diurnal temperature variations as compared to surrounding land (Samuelsson et al., 2010; Notaro et al., 2013; Klaić and Kvakić, 2014), but the high-latitude lakes tend to be cooler than surrounding land in the early summer, and reduce heat flux to the atmosphere during this season (Dutra et al., 2010; Gula and Peltier, 2012; Klaić and Kvakić, 2014). During the cold season, lakes are warmer than the overlying air and would increase surface and atmospheric temperature, reduce atmospheric stability (Notaro et al., 2013), lead to lower sea level pressure, and enhance evaporation and atmospheric moisture (Lofgren, 1997; Scott and Huff, 1997; Notaro et al., 2013). The response of the atmosphere to the lakes during the warm season is generally opposite from the cold season (Notaro et al., 2013). However, the evaluation of the atmosphere–lake coupled model in China has mainly been conducted in Lake Tai, and attempts for other lakes are rare. Therefore, the applicability of the atmosphere–lake coupled model in the two largest freshwater lakes in China is still unknown.

Additionally, the evaluation of the atmosphere–lake coupled model has mainly focused on the LST (Gu et al., 2015, 2016; Martynov et al., 2016), but the meteorological elements may require much more attention when studying lake–atmosphere interaction effects on regional weather and climate. Therefore, the atmosphere–lake coupled model should be assessed based on simulation of the meteorological elements, such as the atmospheric temperature and humidity.

Thus, to evaluate the atmosphere–lake coupled model's performance for meteorological elements in the Lake Poyang and Lake Dongting regions and improve simulations of the lake–atmosphere interactions, a series of experiments without the atmosphere–lake model, with the default atmosphere–lake model, and with the calibrated atmosphere–lake model have been conducted for eight cases with different weather features. Moreover, another two five-month sensitivity experiments using the default and the new calibrated coupled lake models are conducted to evaluate whether the new calibrated coupled lake model works in the Lake Poyang and Lake Dongting regions for long-time simulation.

The remainder of this paper is arranged as follows: Section 2 shows model descriptions, including the coupled lake model and the improved coupled lake model; Section 3 provides experiment design and model configuration, and introduces observed data; Sections 4 and 5 present the results; and Sections 6 and 7 contain the conclusions and discussion, respectively.

2. Model description

2.1 *The coupled lake model*

The lake model coupled in WRF version 3.6 is obtained from the Community Land Model version 4.5 (Oleson et al., 2013) but with some modifications by Gu et al. (2015). It is a one-dimensional mass and energy balance column model partially based on the Hostetler lake model (Hostetler and Bartlein, 1990; Hostetler et al., 1993, 1994), and can simulate 20–25 model layers, including 10 water layers through the depth of the lake, up to 5 snow layers on the lake ice, and 10 soil layers on the lake bottom. The lake model is used with actual lake points and can be used with lake depth derived from the WRF Preprocessing System, or user-defined lake points and lake depth. Besides, the model is independent form the land surface scheme and can thus be used with any land surface model embedded in WRF.

Lake temperature for each water layer is computed by using the 1-D Crank-Nicholson thermal diffusion equation originally from Hostetler and Bartlein (1990). Lake temperature differences, molecular diffusion, and eddy

diffusion are considered for energy transfer calculations within the lake water columns. Eddy diffusivity is parameterized based on Henderson-Sellers (1986), and is set to zero when the lake is frozen. Solar radiation is absorbed at a depth of 0.6-m beneath surface based on the Beer-Lambert Law, and net energy flux at the surface is used as the top boundary condition of thermal diffusion. All energy exchanges, such as radiation, momentum, sensible, and latent heat fluxes, are calculated between the surface and the lower atmosphere. More details about this lake model can be found in Hostetler and Bartlein (1990), Subin et al. (2012), and Gu et al. (2015).

2.2 *Calibrations of the coupled lake model*

Deng et al. (2013) and Gu et al. (2014) performed offline tests of the Hostetler-based lake model in Lake Tai and found that it was incapable to reproducing the temperatures with default parameter settings. Gu et al. (2015) demonstrated that the Hostetler-based lake model generated strong LST biases (up to ± 20°C) in Lake Superior. Stepanenko et al. (2013) and Xu et al. (2016) also found similar results for Lake Kossenblatter in Germany and Lake Erhai in China, respectively. However, this lake model's simulated biases can successfully be reduced by calibrating the fraction of solar radiation absorbed by the lake water, the roughness length, and the light extinction coefficient. Therefore, the lake model's failure to reproduce temperatures may be related to lake physical parameters such as roughness length and water turbidity, which would affect near-surface solar radiation absorption and solar energy remaining in the upper water layer. Lake Poyang and Lake Dongting are both large and shallow lakes in the middle–lower Yangtze plain just like Lake Tai; thus in this study, we calibrate some parameters of the lake model based on Gu et al. (2014, 2016) to improve lake–atmosphere interaction simulations. First, the fraction of solar radiation absorbed by the lake water is changed from 0.4 to 0.8. Second, the light extinction coefficient is increased by a factor of 3 to produce a new coefficient of 3.5775. Lastly, the visible part of shortwave radiation is changed, which is originally absorbed below a 0.6-m depth in lake, and now is absorbed immediately beneath the surface. Additionally, we modify the momentum, thermal, and water vapor roughness lengths, which have original values of 0.001, to 3.3×10^{-4} m, 1.9×10^{-6} m, and 3.9×10^{-8} m, respectively (Xiao et al., 2013), based on the ecological environment.

3. Experiment design and observed data

3.1 *Experiment design*

To evaluate the performance of the original atmosphere–lake coupled model and the new calibrated coupled lake model in the Lake Poyang and Lake Dongting regions, eight cases with different weather features are chosen. Cases 1–4 are used to test whether the default coupled atmosphere–lake model works compared without the coupled atmosphere–lake model and to evaluate the new calibrated model. And cases 5–8 are used to verify the results and applicability of the new calibrated model.

Table 1 lists the eight cases, and Fig. 1 shows cumulative precipitation during the simulation time for each case. Case 1 (02P, here "02" refers to the month and "P" indicates that there is precipitation during the case) occurs in winter and there is precipitation over the Lake Poyang and Lake Dongting regions. Case 2 (02N, here "N" indicates there is no precipitation during the case) occurs also in winter but there is no precipitation over the Lake Poyang and Lake Dongting regions. Case 3 (06P) occurs in summer with precipitation over the Lake Poyang and Lake Dongting regions. Case 4 (08N) occurs in summer and there is no precipitation over the Lake Poyang and Lake Dongting regions. We use these four cases to evaluate the performance of both the default atmosphere–lake coupled model and the new calibrated model. Cases 5–8 (01P, 01N, 07P, and 07N) have similar characteristics to cases 1–4 (Table 1 and Fig. 1). We use these cases to verify the results and applicability of the new calibrated model. Three experiments are conducted for each case. The first is conducted without the atmosphere–lake coupled model during the simulation (NO-

Table 1. List of cases used in the study. The number refers to the month and the letter indicates presence or absence of precipitation during the case ("P" = precipitation, "N" = no precipitation)

Case (No.)	Simulation time	Season	Precipitation
Case 1 (02P)	1200 UTC 8 to 0000 UTC 12 February 2011	Winter	Yes
Case 2 (02N)	1200 UTC 4 to 0000 UTC 8 February 2011	Winter	No
Case 3 (06P)	1200 UTC 8 to 0000 UTC 12 June 2011	Summer	Yes
Case 4 (08N)	1200 UTC 14 to 0000 UTC 18 August 2011	Summer	No
Case 5 (01P)	1200 UTC 1 to 0000 UTC 5 January 2011	Winter	Yes
Case 6 (01N)	1200 UTC 8 to 0000 UTC 12 January 2011	Winter	No
Case 7 (07P)	1200 UTC 21 to 0000 UTC 25 July 2011	Summer	Yes
Case 8 (07N)	1200 UTC 24 to 0000 UTC 28 July 2011	Summer	No

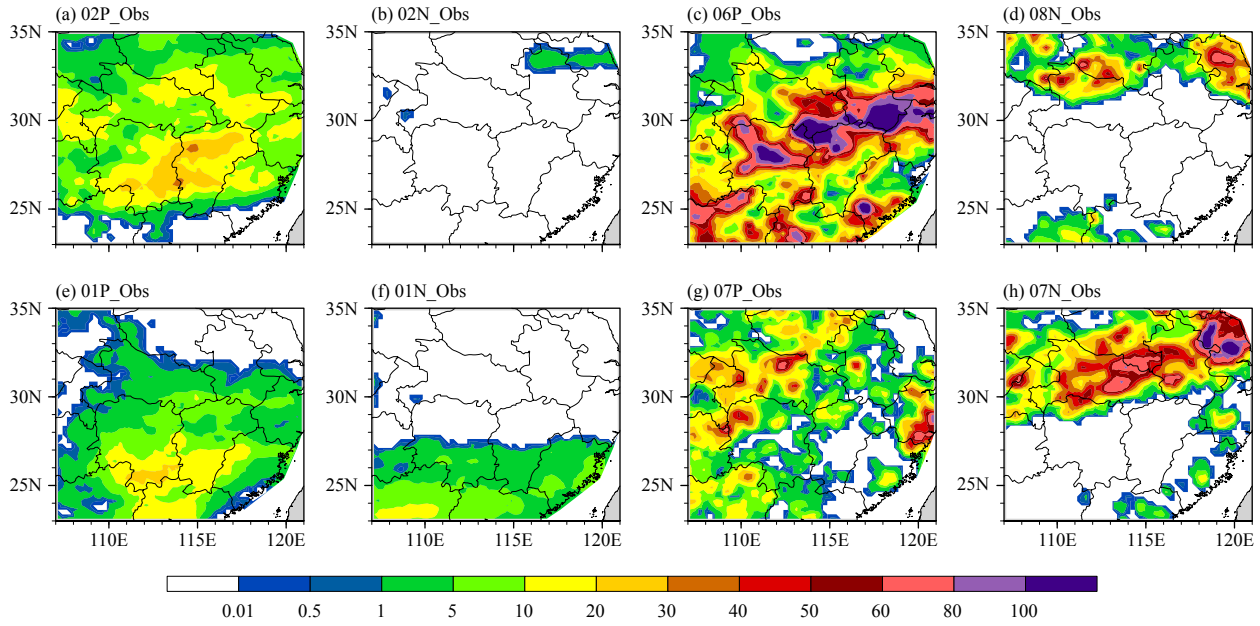

Fig. 1. Accumulated precipitation (mm) obtained from the 0.25°-resolution prepcitation dataset of the NMIC of China during the simulation time for (a–h) cases 1–8.

LAKE experiment), the second is conducted with the default atmosphere–lake coupled model during the simulation (OLD experiment), and the third is conducted with the new calibrated atmosphere–lake coupled model during the simulation (NEW experiment).

3.2 *Model configuration*

The model used in this study is the WRF model version 3.7.1. We obtain the initial and boundary conditions for the large-scale atmospheric fields and the initial soil parameters (soil water, moisture, and temperature) from the third-generation ECMWF reanalysis product-Interim (ERA-Interim) data. We employ two nested domains centered at 30°N, 105°E with grid numbers and spacings of 261 × 221 and 306 × 306, and 30 and 6 km (Fig.2a), respectively. Each domain has 35 terrain-following eta vertical coordinate levels extending from the surface to 50 hPa.

The main physical options used here include the WRF single-moment 6-class microphysics scheme (Hong and Lim, 2006), the new version of rapid radiative transfer model longwave radiation and shortwave radiation scheme (Mlawer et al., 1997), the Noah-MP (multi-parameterization) land-surface model (Niu et al., 2011), and the Yonsei University planetary boundary layer scheme (Noh et al., 2003). Only the outer domain employ the Kain–Fritsch (new Eta) cumulus parameterization scheme (Kain, 2004). In this study, we run each experiment for 84 h and output simulation results hourly. The initial 12 hours are considered as a spin-up period and excluded from the analysis.

3.3 *Observed data*

The observations used for comparisons with temperature and dew-point temperature at 2 m above the ground level are obtained from every three hours' conventional ground and sounding data. We select 16 stations (Fig. 2c), including three near Lake Poyang (stations 58506, 58606, and 58519), four near Lake Dongting (stations 57574, 57584, 57671, and 57673), three between Lake Poyang and Lake Dongting (stations 57696, 58600, and 58507), three in the upwind region of Lake Dongting (stations 57562, 57662, and 57669), and three in the downwind region of Lake Poyang (stations 58622, 58527, and 58531).

In this study, we use two types of precipitation datasets. The first precipitation dataset, obtained from the National Meteorological Information Center of China (NMICC), is a real time analysis system with a 0.25° resolution and daily precipitation over China (1st edition) and is used in Fig. 1 to confirm the presence of precipitation over the Lake Poyang and Lake Dongting regions. The second precipitation dataset, which is also obtained from NMICC, is an hourly 0.1° × 0.1° merged precipitation product used for comparison with model simulations. For ease of comparison, we select six regions (Fig. 2b,c), i.e., py1 (28.3°–30.3°N, 115.5°–117.5°E), dt1 (28.3°–30.3°N, 111.5°–113.5°E), py2 (27°–31°N, 114°–118°E),

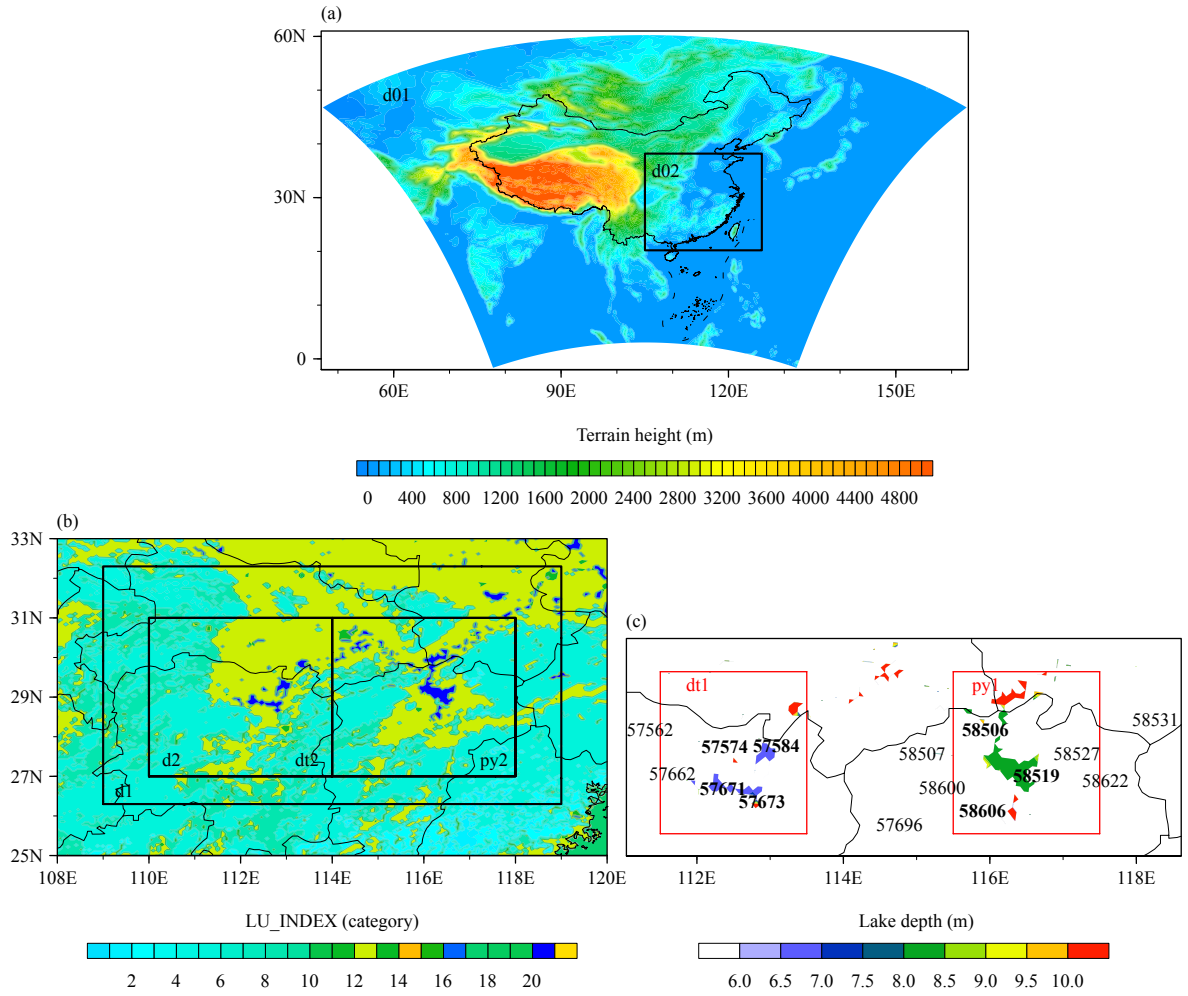

Fig. 2. (a) The Weather Research and Forecasting (WRF) model domain. (b) The blue areas indicate Lake Poyang and Lake Dongting. The area of d2 in (b) is the sum of py2 and dt2, and the area of d1 is larger than d2. (c) Lake depths and observation stations in the Lake Poyang and Lake Dongting areas. The black solid lines in (b) and the red solid lines in (c) enclose the analysis areas of precipitation. The sites in bold numbers are the observatories around the lake, and the others are observatories farther away from the lake.

dt2 (27°–31°N, 110°–114°E), d2 (27°–31°N, 110°–118°E), and d1 (26.3°–32.3°N, 109°–119°E).

4. Results

4.1 *Performance of the default and the new calibrated coupled lake model*

4.1.1 *Temperature and dew-point temperature at 2 m*

The evolution of simulated biases of 2-m temperature and dew-point temperature for cases 1–4 is shown in Figs. 3–6. For illustration purposes, we only show snapshots of simulated biases at stations 58606, 57584, 57662, 58507, and 58600. For case 1 (02P), all the three experiments have simulated 2-m temperature and dew-point temperature biases, and these biases show obvious diurnal variation (Fig. 3). The biases of the NOLAKE and OLD experiments mainly show no differences for 2-m temperatures at all stations; however, the OLD experiment shows a lightly larger bias at station 58606 at 0500 BT (Beijing Time) 10 February. On the other hand, the 2-m dew-point temperature has noticeably higher biases at all stations except station 57662 for the OLD experiment than the NOLAKE experiment, and these biases are relatively larger at stations near lakes than at stations far away from the lakes. The NEW experiment has a better performance for 2-m temperatures at stations 58606 and 58507 and much better 2-m dew-point temperatures at stations near the lakes. At station 58606, the 2-m dew-point temperature bias is reduced by nearly 1°C.

For case 2 (02N), the simulated 2-m temperature biases show nearly no differences among the three experiments except at station 57584 (Fig. 4). Although the NEW experiment performs better for 2-m temperature at station 57584 sometimes, the OLD experiment shows a smaller bias overall. Additionally, 2-m temperature biases at station 58606 are also different, but the differ-

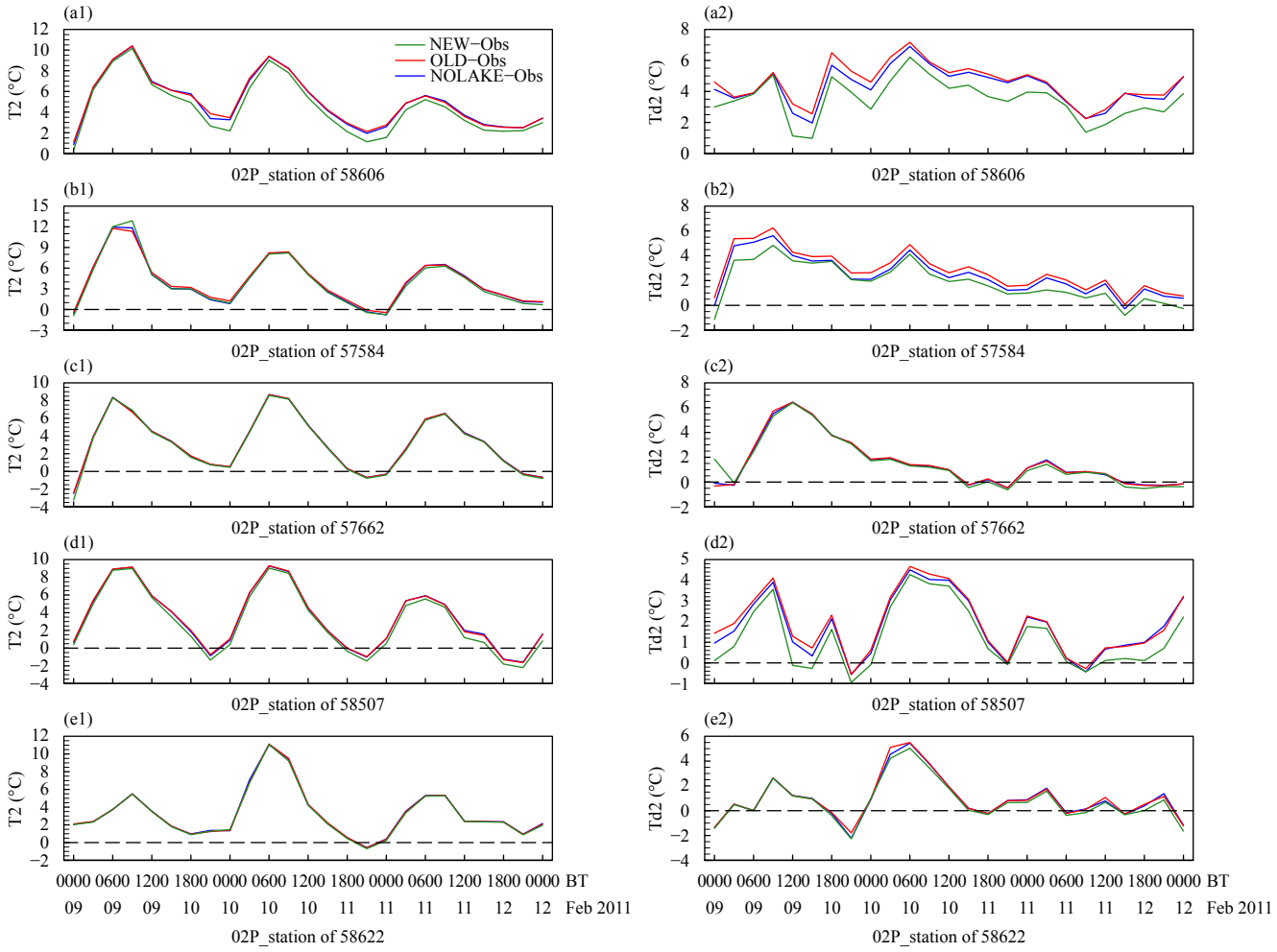

Fig. 3. Evolutions of simulated biases of (a1–e1) 2-m temperature (T2) and (a2–e2) dew-point temperature (Td2) at stations 58606, 57584, 57662, 58507, and 58622 for case 1.

ence is not obvious and thus it is hard to say which experiment performs better at this station. However, simulated 2-m dew-point temperature biases are rather different among the three experiments except at station 58622. The OLD experiment performs worst, with 2-m dew-point temperature biases sometimes reaching 2°C. The NEW experiment performs much better than the other two for 2-m dew-point temperature, especially at stations near the lakes.

For case 3 (06P), Fig. 5 shows that simulated 2-m temperature and dew-point temperature bias has big differences among the three experiments and five selected stations. At station 57584, the NEW experiment performs best during the first simulated day, and the NOLAKE experiment performs worst for both 2-m temperature and dew-point temperature. However, during the last two simulated days, simulated biases are opposite, and the simulated 2-m temperature and dew-point temperature biases of the NOLAKE experiment are close to zero. Further analysis will be needed to draw conclusions about which experiment performs better at the other stations.

For case 4 (08N), simulated 2-m temperature and dew-point temperature biases show differences among the three experiments; however, the differences are relatively small except at station 57584 (Fig. 6). At station 57584, the NEW experiment performs much better for 2-m temperature and the NOLAKE experiment shows the largest bias. For 2-m dew-point temperature, the coupled lake model reduces biases almost 2°C compared to the NOLAKE experiment during the whole simulated time, and the NEW experiment shows relatively smaller bias. At station 58606, all three experiments perform similarly except during the last 12 simulated hours. During this time, the NOLAKE and OLD experiments both have smaller 2-m temperature biases, with the 2-m dew-point temperature bias of the OLD experiment being the smallest.

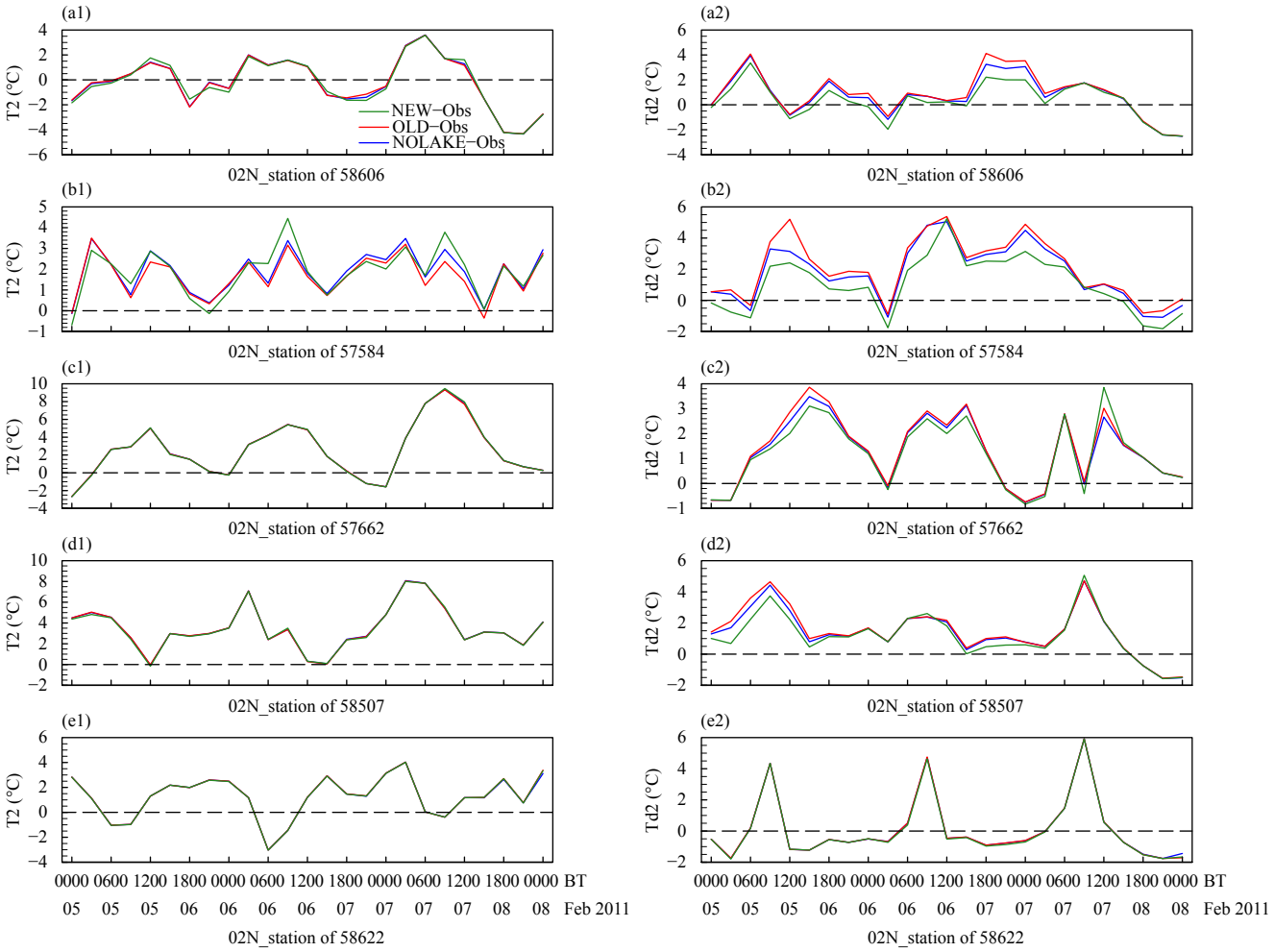

Fig. 4. As in Fig. 3, but for case 2.

To illustrate which performs better, we calculate the absolute mean simulated biases during the simulated time for 2-m temperature and dew-point temperature. Figures 7 and 8 show the differences of absolute mean simulated biases between the three experiments. In these figures, the blue line represents the difference between the NOLAKE and OLD experiments, which is calculated by subtracting the absolute value of the mean simulated biases during the simulated time for the NOLAKE experiment from that for the OLD experiment. When the blue line is greater than zero, OLD experiment has larger mean simulated biases than the NOLAKE experiment, indicating that the NOLAKE experiment performs better than the OLD experiment and that the coupled lake model makes no difference here. The red line represents the difference between the OLD and NEW experiments and the black line represents the difference between the NOLAKE and NEW experiments. When the red and black lines are less than zero, then the NEW experiment performs better than the OLD and NOLAKE experiments.

In Fig. 7a, the blue line is greater than zero at almost all stations, whereas the red and black lines are below zero. This indicates that the NOLAKE experiment performs better than the OLD experiment and that the NEW experiment performs better than the OLD and NOLAKE experiments at all stations for 2-m temperature in case 1 (02P). For case 2 (02N), the NOLAKE and OLD experiments show nearly no difference over the Lake Poyang region and at stations far from the lakes; however, over the Lake Dongting region, the OLD experiment performs best. For case 3 (06P), the NOLAKE experiment performs slightly better than the OLD experiment and the NEW experiment performs best over the Lake Poyang region, at station 57584, and at stations far from the lakes. For case 4 (08N), the three experiments show nearly no performance differences over the Lake Poyang region and at stations far from the lakes. Over the Lake Dongting region, the OLD and NEW experiments have significantly reduced 2-m temperature biases. The decreases of the absolute mean simulated 2-m temperature

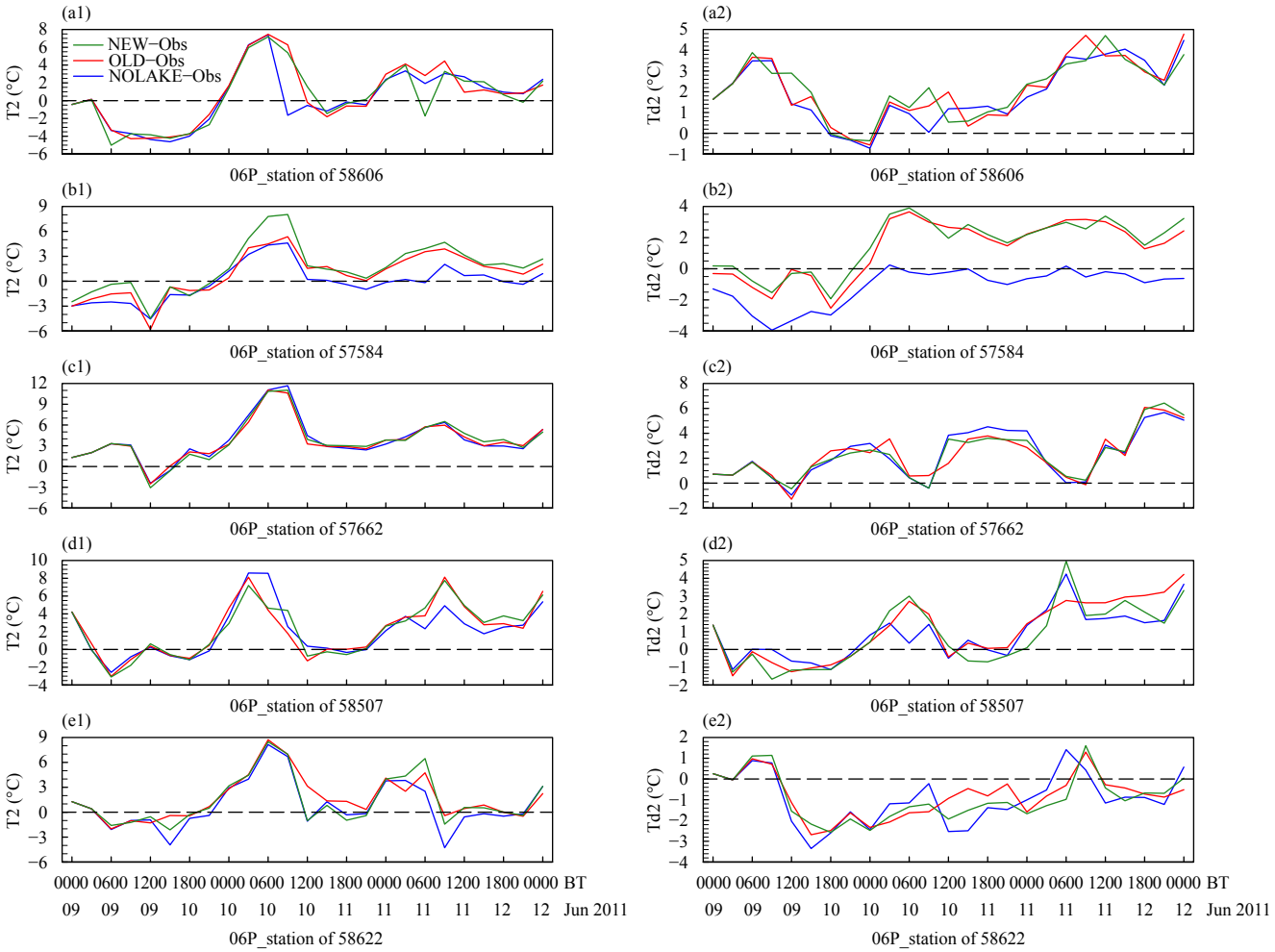

Fig. 5. As in Fig. 3, but for case 3.

biases are close to 2.0 and 4.0°C for the OLD and NEW experiments, respectively, compared with the NOLAKE experiment.

For case 1 (02P) and case 2 (02N), the NOLAKE experiment performs better than the OLD experiment, and the NEW experiment performs best at all stations for 2-m dew-point temperature, especially over the Lake Dongting region (Fig. 8). However, for case 3 (06P), it is difficult to draw a conclusion about which experiment performs better. For case 4 (08N), the three experiments show no obvious performance differences at stations far from the lakes; however, the OLD and NEW experiments both show significantly reduced 2-m dew-point temperature biases over the Lake Dongting region. Decreases of the absolute mean simulated 2-m dew-point temperature biases reach 3.0°C for the OLD and NEW experiments compared with the NOLAKE experiment. Over the Lake Poyang region, the NOLAKE experiment performs slightly better than the OLD experiment. In addition, the NEW experiment performs best at all stations.

4.1.2 *Surface pressure and wind speed at 10 m*

Differences in absolute mean simulated biases for the surface pressure and 10-m wind speed between the three experiments are shown in Figs. 9, 10. Figure 9 shows that the NOLAKE experiment performs slightly better than the OLD experiment and that the NEW experiment performs better than the OLD and NOLAKE experiments at all stations (except for stations near Lake Poyang) for surface pressure for case 1 (02P). For case 4 (08N), the NEW experiment has the best performance for surface pressure, followed by the OLD experiment, and NOLAKE experiment has the largest bias over the Lake Dongting region. For case 2 (02N) and case 3 (06P), the NEW experiment performs best in the downwind region of Lake Poyang and region between Lake Poyang and Lake Dongting.

For 10-m wind speed, Fig. 10 shows that the NOLAKE experiment performs slightly better than the OLD experiment and that the NEW experiment performs best for case 1 (02P) and case 3 (06P). For case 2 (02N), the

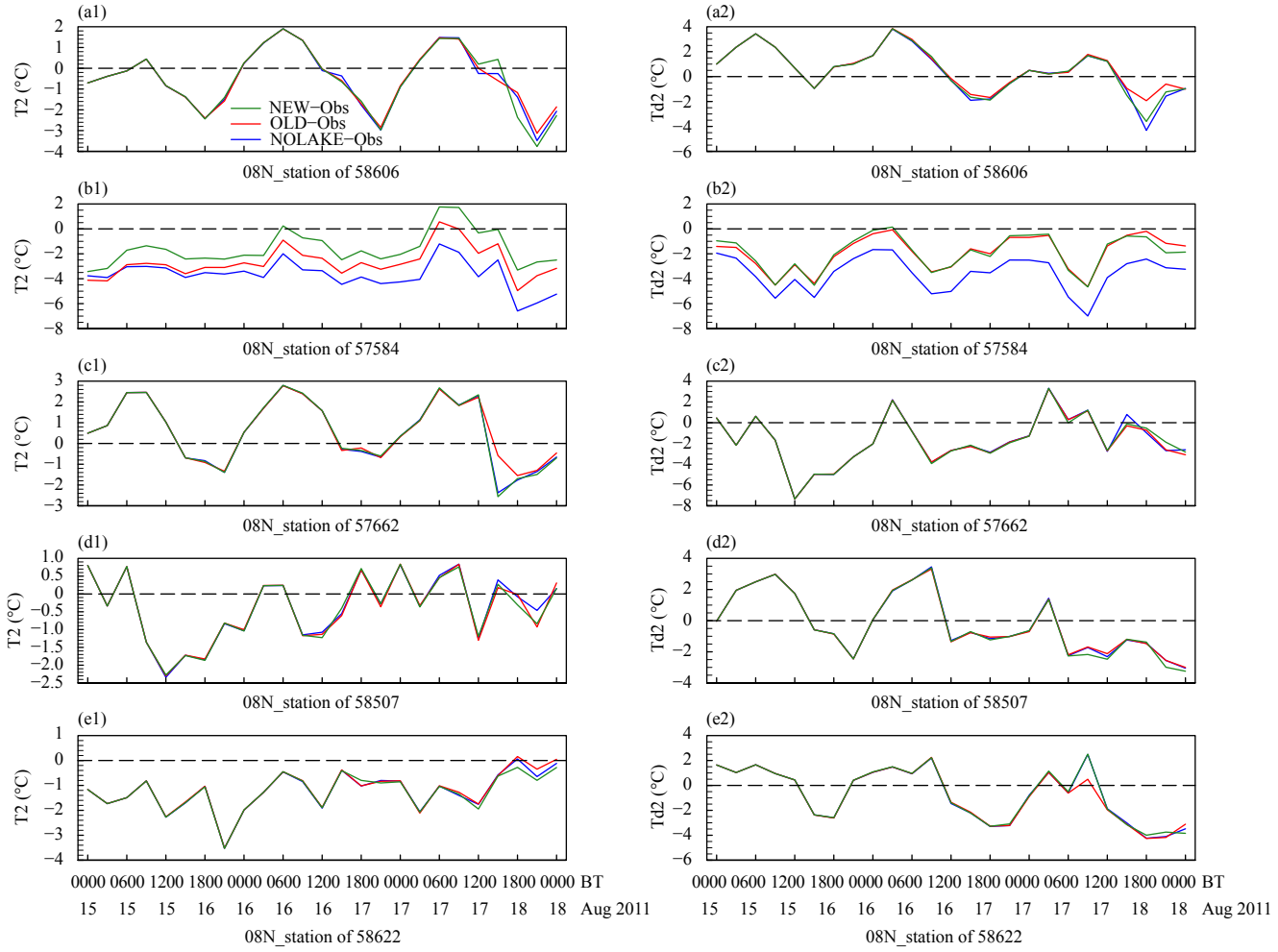

Fig. 6. As in Fig. 3, but for case 4.

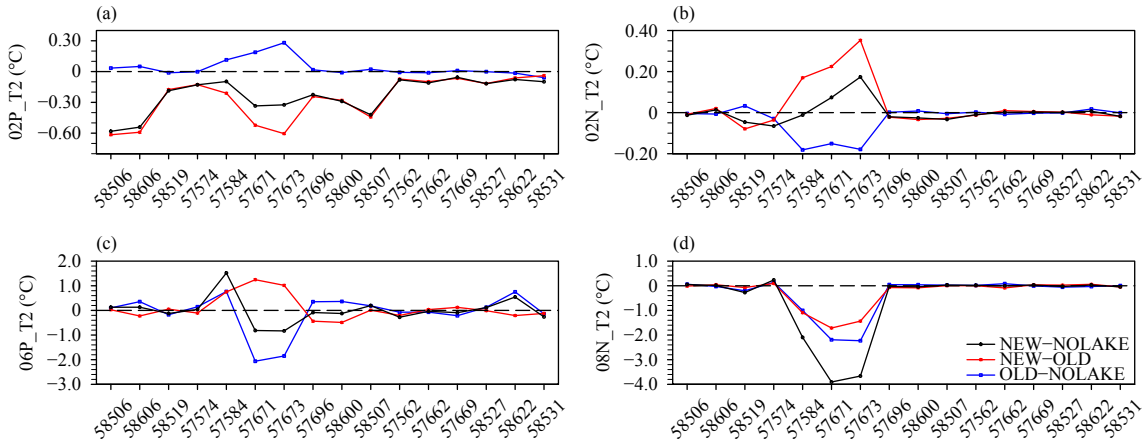

Fig. 7. Differences in the absolute mean simulated biases during the simulated time for 2-m temperature at all selected stations for (a–d) cases 1–4.

OLD experiment performs better than the NEW experiment over the Lake Dongting region, followed by the NEW experiment. The NOLAKE experiment has the largest bias. The NEW experiment performs better than the OLD experiment over the Lake Poyang region, followed by the NOLAKE experiment. For case 4 (08N), the OLD experiment performs better than the NEW and NOLAKE experiments.

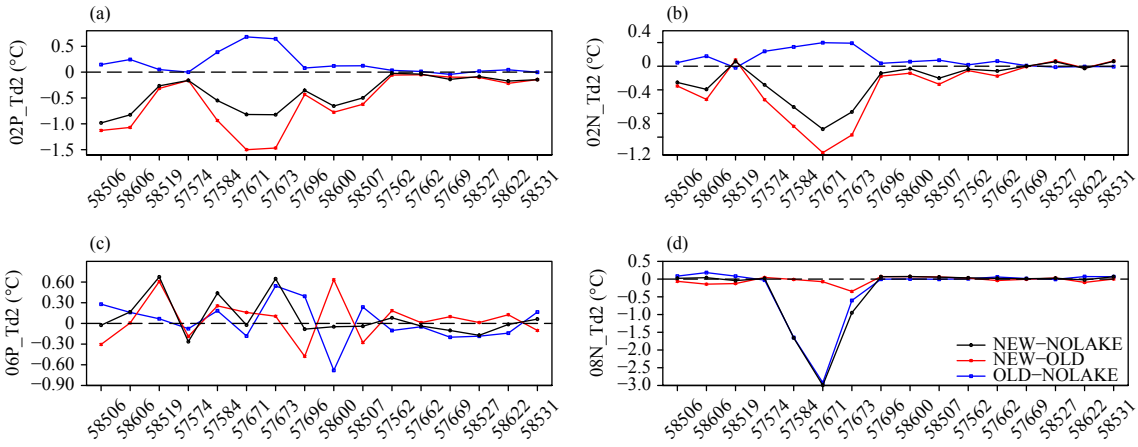

Fig. 8. As in Fig. 7, but for 2-m dew-point temperature at all selected stations for (a–d) cases 1–4

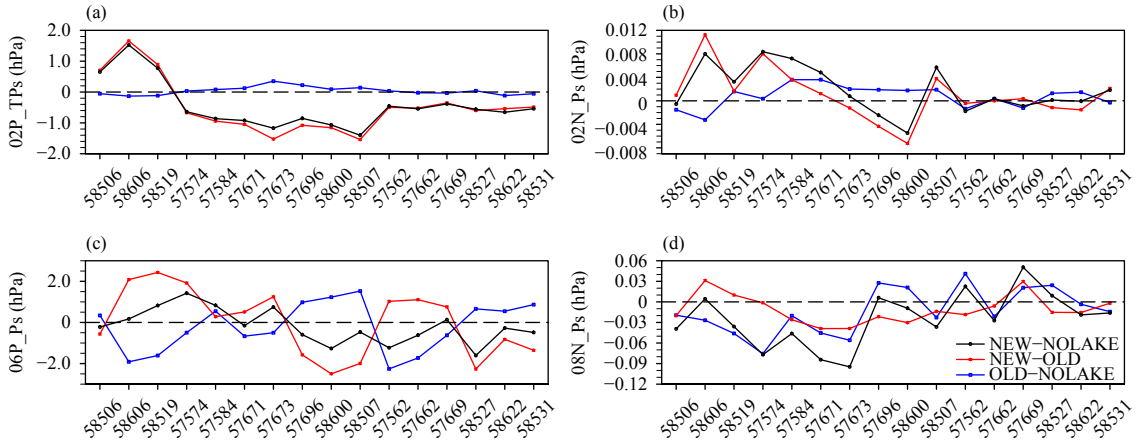

Fig. 9. As in Fig. 7, but for the surface pressure at all selected stations for (a–d) cases 1–4.

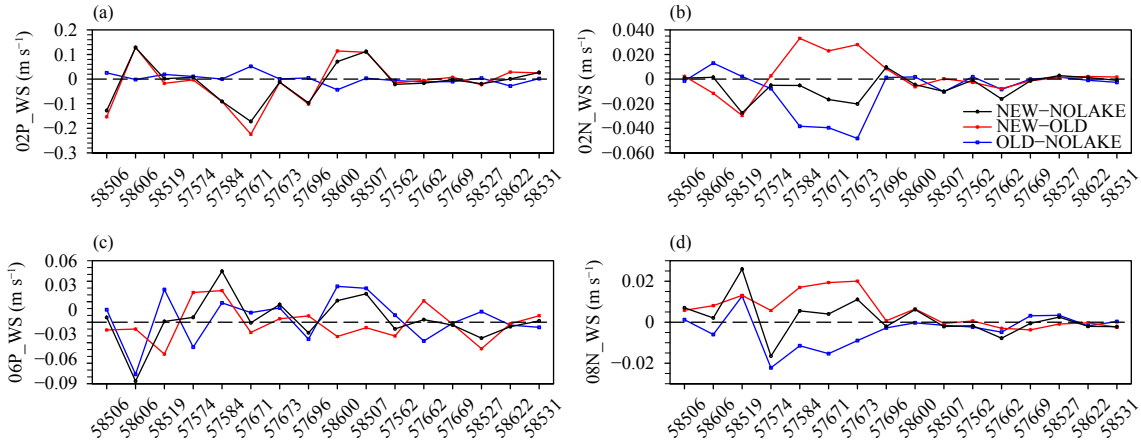

Fig. 10. As in Fig. 7, but for the 10-m wind speed for (a–d) cases 1–4.

4.1.3 *Precipitation*

The differences in mean simulated hourly precipitation biases during the simulated time averaged in the selected areas among the three experiments (NOLAKE, OLD, and NEW) for case 1 (02P) and case 3 (06P) are listed in Table 2. Generally speaking, the difference in absolute mean simulated biases between the NOLAKE and OLD experiments for case 1 (02P) is small, but the values are all greater than zero, which indicates that the NOLAKE experiment performs better than the OLD ex-

Table 2. Differences in mean simulated biases (mm) during the simulated time for hourly precipitation averaged over regions py2, dt2, d2, and d1 for cases 1 and 3. "OLD–NOLAKE" is the difference between the NOLAKE and OLD experiments, "NEW–OLD" is the difference between the OLD and NEW experiments, and "NEW–NOLAKE" is the difference between the NOLAKE and NEW experiments

Case		py2	dt2	d2	d1
02P	OLD–NOLAKE	0.016	0.078	0.031	0.028
	NEW–OLD	–0.004	–0.313	–0.155	–0.152
	NEW–NOLAKE	0.012	–0.235	–0.124	–0.124
06P	OLD–NOLAKE	–8.288	–0.231	–4.260	0.445
	NEW–OLD	–0.926	–2.636	–1.781	–1.507
	NEW–NOLAKE	–9.214	–2.867	–6.040	–1.062

periment. The difference between the NEW and OLD experiments are larger and the values are less than zero. This indicates that the NEW experiment performs better than the OLD experiment for those four areas, especially in areas dt2, d2, and d1. Except for area py1, the differences between the NEW and NOLAKE experiments are also all less than zero. Therefore, the NEW experiment performs better, too.

In addition, Table 2 also shows differences in absolute mean simulated biases among the three experiments for case 3 (06P) are much larger than for case 1 (02P). This may be because of summer precipitation in the Yangtze River delta and southern China is affected by the East Asian summer monsoon, which is accompanied by seasonal variations in heavy precipitation associated with large-scale circulation, and is thus much larger than winter precipitation. Another reason could be that summer precipitation is usually caused by local convection systems that are sensitive to the land–lake breeze, whereas winter precipitation is typically due to large-scale circulation, thus making the influence of land–lake breeze rather small. Therefore, summer precipitation is sensitive to lake parameterization.

In areas py2, dt2, and d2, the OLD experiment performs better than the NOLAKE experiment because the difference is less than zero. The differences between the NEW and OLD experiments and between the NEW and NOLAKE experiments are all less than zero, which indicates that the NEW experiment performs better than the OLD and NOLAKE experiments in these four areas. Therefore, the NEW experiment performs best and adopting the new calibrated model in the simulation process would reduce simulated precipitation biases for case 3 (06P).

Here, we choose case 3 (06P) as an example and the Lake Dongting region as the typical area to analyze why the NEW experiment performs better than the NOLAKE and OLD experiments. Figure 11 shows that all the three experiments have dry biases for precipitation over the Lake Dongting region; however, the OLD and NEW experiments can both simulate more precipitation than the NOLAKE experiment, with regional averaged values of 6.12 and 7.33 mm, respectively. And although not obvious, the NEW experiment simulates more precipitation than the OLD experiment, with a regional averaged value of 1.21 mm. Thus, the NEW experiment can decrease dry biases of the NOLAKE and OLD experiments. Further, we analyze differences in sensible and latent heat fluxes, surface skin temperature, air temperature, zonal and meridional wind at the lowest model level, land–air temperature contrast, and the three-day accumulated precipitation for case 3 (06P) averaged over the Lake Dongting region (Table 3). Compared to the NOLAKE experiment, the OLD and NEW experiments can increase sensible and latent heat fluxes, thus raising the surface skin and air temperatures. But the increase of surface skin temperature is larger than that of air temperature, resulting in a corresponding increase in land–air temperature contrast. Moreover, the lake–land surface temperature differences can generate lake breezes, which strengthen zonal winds but weaken meridional winds. Influenced by thermal and dynamical factors together, the planetary boundary layer height increases, indicating that the OLD and NEW experiments simulate a more unstable lower atmosphere, which can strengthen low-level convergences, promote thermal convective activities, and ultimately intensify precipitation over the Lake Dongting region. Comparing the NEW and OLD experiments, it can be found that the NEW experiment can increase sensible heat flux and surface skin temperature but decrease latent heat flux and air temperature. Similarly, lake–land surface temperature difference increases with enhanced zonal winds and weakened meridional winds, resulting in increased planetary boundary layer height. Thus, the NEW experiment also simulates a more unstable lower atmosphere than the OLD experiment, which helps intensify precipitation and reduce dry biases.

4.2 *Applicability of the calibrated coupled lake model*

To verify these results and the applicability of the new calibrated model, we choose another four cases (cases 5–8 in Table 1) and conduct the same three experiments for each case. Figure 12 shows that the blue line is greater than zero at almost all stations and that the red and black

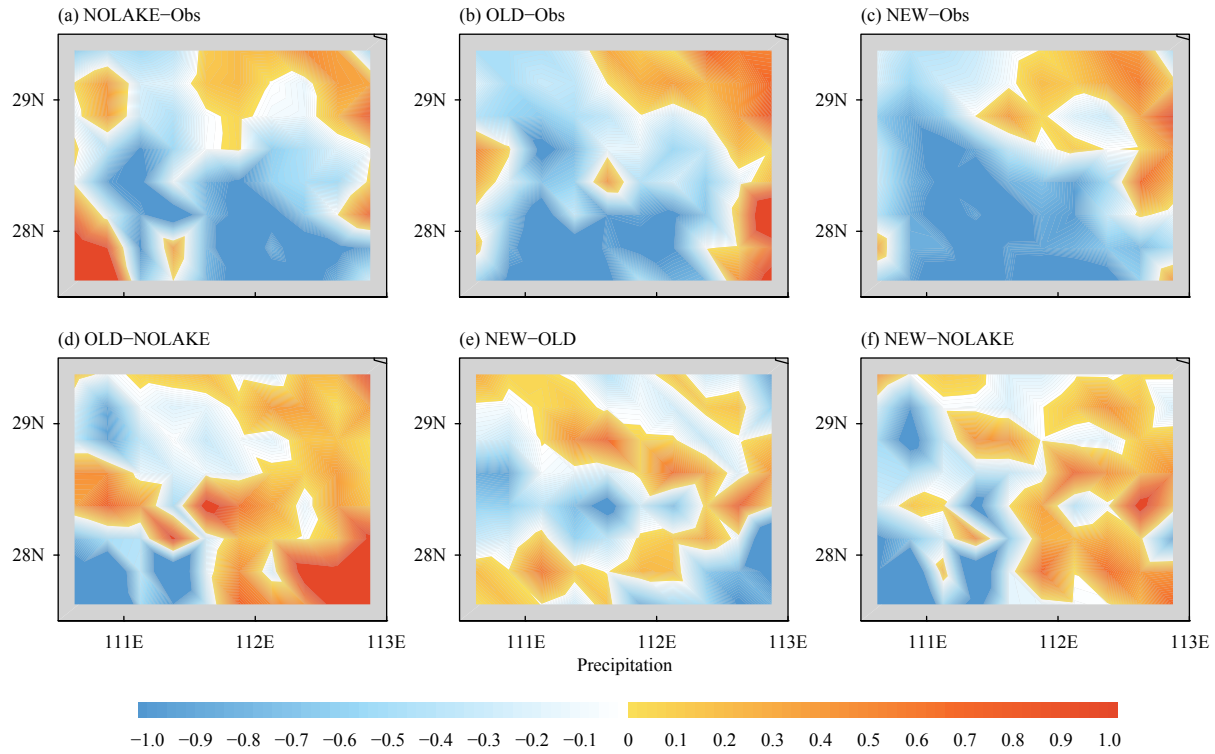

Fig. 11. (a–c) Biases and (d–f) differences of the three-day accumulated precipitation (mm h^{-1}) for case 3 (06P) for the three experiments (NOLAKE, OLD, and NEW) in the Lake Dongting region.

Table 3. Difference in the averaged simulated sensible heat flux (HFX), latent heat flux (LH), surface skin temperature (TSK), air temperature (Tc), zonal wind (U1), and meridional wind (V1) at the lowest model level, land–air temperature contrast (TSK–Tc), planetary boundary layer height (PBLH), and three-day accumulated precipitation for case 3 (06P) averaged over the Lake Dongting region

	LH (W m^{-2})	HFX (W m^{-2})	TSK (°C)	Tc (°C)	U1 (m s^{-1})	V1 (m s^{-1})	TSK–Tc (°C)	PBLH (m)	Precipitation (mm)
OLD–NOLAKE	15.63	5.30	1.53	0.42	0.05	–0.25	1.12	88.99	6.12
NEW–OLD	4.31	–0.18	0.29	–0.06	0.16	–0.56	0.34	68.38	1.21
NEW–NOLAKE	19.94	5.12	1.82	0.36	0.21	–0.80	1.46	157.38	7.33

lines are all less than zero. This means that the NOLAKE experiment performs better than the OLD experiment and that the NEW experiment performs better than the OLD and NOLAKE experiments at all stations for 2-m temperature for case 5 (01P). For case 6 (01N), there is nearly no difference for the NOLAKE and OLD experiments; however, the NEW experiment performs better over the Lake Poyang region. Over the Lake Dongting region, results vary by station and the NEW experiment performs relatively better overall. For case 7 (07P) and case 8 (07N), the three experiments show nearly no difference over the Lake Poyang region and at stations far from the lakes. Over the Lake Dongting region, the OLD and NEW experiments show significantly reduced 2-m temperature biases.

For case 5 (01P) and case 6 (01N), the NOLAKE experiment performs better than the OLD experiment and the NEW experiment performs best at all stations for 2-m dew-point temperature, especially over the Lake Dongting region (Fig. 13). For case 7 (07P) and case 8 (07N), the OLD and NEW experiments both show significantly reduced 2-m dew-point temperature biases over the Lake Dongting region. Overall, the NEW experiment performs best at all stations for these two cases.

For surface pressure, Fig. 14 shows that the NOLAKE experiment performs better than the OLD experiment and that the NEW experiment performs best at all stations except for those in the Lake Poyang region for case 5 (01P). For case 6 (01N), the NEW experiment performs best in region upwind of Lake Dongting, downwind of Lake Poyang, and between Lake Poyang and Lake Dongting. For case 7 (07P) and case 8 (07N), the NEW experiment performs best over the Lake Poyang and Lake Dongting regions. For 10-m wind speed (Fig. 15), the NEW experiment performs best for case 5 (02P) and case 6 (02N) (Fig. 14). But for case 7 (06P) and case 8 (08N), it is hard to say which experiment performs better.

For precipitation, the difference in absolute mean sim-

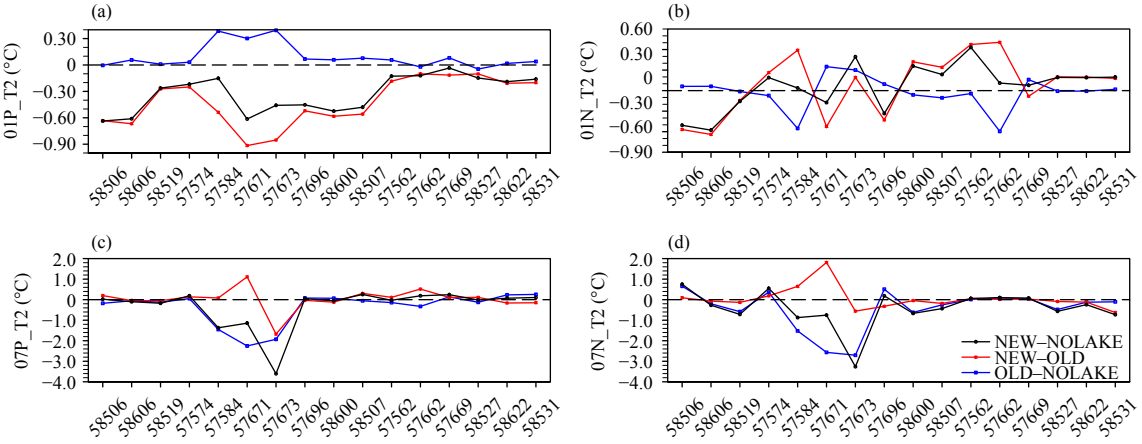

Fig. 12. As in Fig. 7, but for (a–d) cases 5–8.

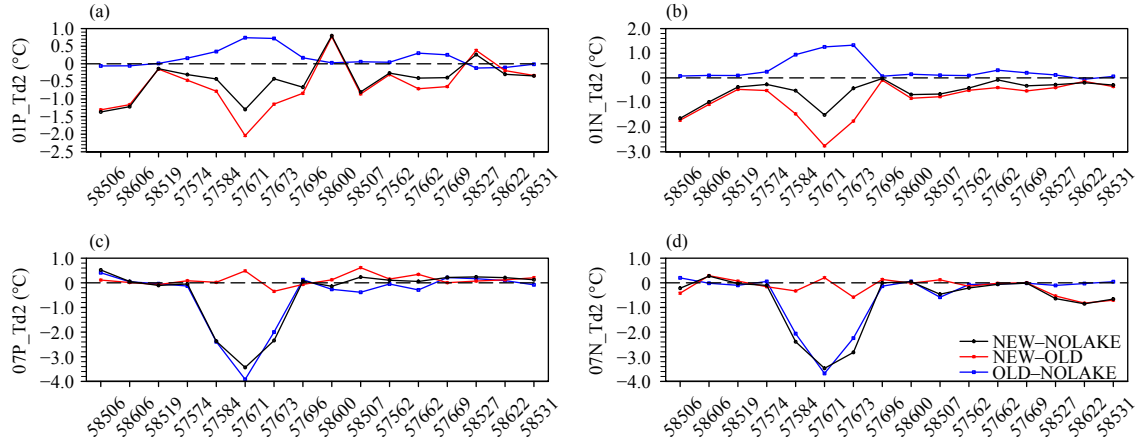

Fig. 13. As in Fig. 8, but for (a–d) cases 5–8.

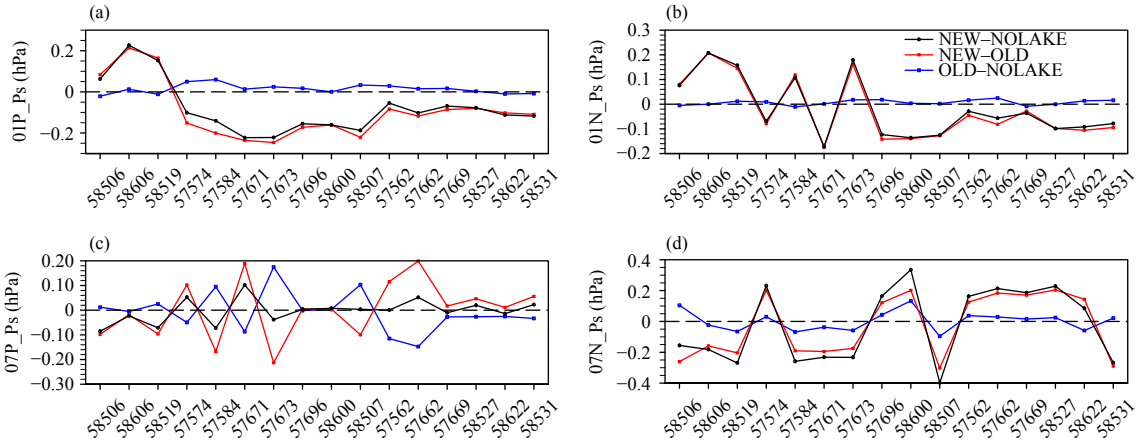

Fig. 14. As in Fig. 9, but for (a–d) cases 5–8.

ulated biases between the NOLAKE and OLD experiments for case 5 (01P) is also rather small and the NOLAKE experiment performs better than the OLD experiment in areas d2 and d1; however, the results are opposite in areas py2 and dt2 (Table 4). The relative differences in absolute mean simulated biases among the NEW, OLD, and NOLAKE experiments are larger and almost less than zero, indicating that the NEW experiment performs best in areas dt2, d2, and d1. For case 7 (07P), the NEW experiment performs best and the OLD

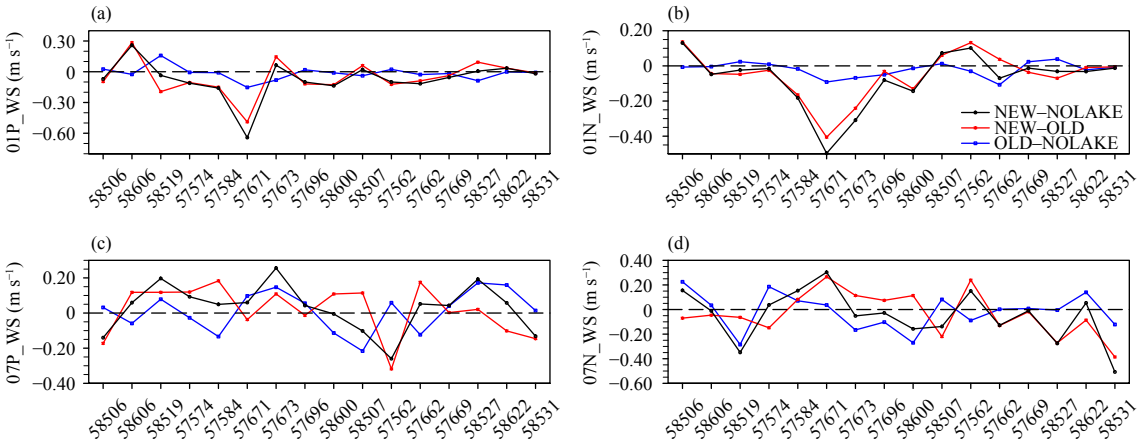

Fig. 15. As in Fig. 10, but for (a–d) cases 5–8.

Table 4. As in Table 2, but for cases 2 and 4

Case		py2	dt2	d2	d1
01P	OLD–NOLAKE	–0.081	–0.013	0.034	0.041
	NEW–OLD	0.178	–0.437	–0.308	–0.174
	NEW–NOLAKE	0.097	–0.451	–0.274	–0.134
07P	OLD–NOLAKE	0.379	0.375	0.002	–0.544
	NEW–OLD	–0.204	–0.026	–0.089	–0.209
	NEW–NOLAKE	0.176	0.350	–0.087	–0.753

experiment performs worst.

Moreover, two sensitivity experiments lasting five months (1 October 2010 to 1 March 2011) are conducted by using the default and new calibrated models to evaluate whether the new calibrated model works in the Lake Poyang and Lake Dongting regions for long-term simulation. The results show that the new calibrated model has a relatively lower root mean square error and higher correlation coefficient for daily average temperature and relative humidity at 2 m, and thus still performs better than the default model over the long-term.

5. Discussion

For the precipitation cases (e.g., 02P and 01P), positive temperature deviations are very large, especially for daytime temperature; therefore, simulation results increase diurnal temperature variations. In the no precipitation cases, simulated temperature is relatively accurate; however, there are still positive daytime and negative nighttime biases. This may be because the model's parameterization schemes, such as the boundary layer and radiation schemes, and land surface parameters (e.g., terrain height, vegetation coverage, and surface albedo) are unsuitable. Li et al. (2014) explored the effects of radiation physics on precipitation and found that radiation physics schemes produced biases in radiation fluxes, leading to variations in the meridional gradient of surface temperature, which would affect circulation and precipitation. Xu et al. (2016) indicated that four different radiation parameterization schemes reproduced total solar radiation well on clear days but generated large bias on cloudy days. Moreover, unrealistic vegetation cover and surface albedo would cause systematic air temperature biases in the simulation and updating vegetation cover or albedo in the model using satellite products can decrease such biases (Meng et al., 2014, 2018).

Precipitation cases involve more physical processes than cases without precipitation. Here, we take the radiation parameterization scheme as an example. Result shows that observed temperature has no diurnal variation for precipitation cases (02P, 01P, and 06P); however, daily variations of simulated temperature and net radiation are very obvious, which is very similar to cases without precipitation (02N and 08N) (figure omitted). This indicates that simulated radiation may contain large positive biases for rainy days (Li et al., 2014; Xu et al., 2016), which can eventually result in positive sensible heat flux and temperature biases.

For winter precipitation cases (02P), simulated temperature usually shows positive biases, and the new calibrated model would reduce sensible and latent heat fluxes, reducing the simulated temperature and its biases. For winter without precipitation cases (02N), the new calibrated model reduces simulated temperature and its biases by decreasing the sensible and latent heat fluxes, but increases the simulated temperature and its biases by

increasing the latent heat flux. In summer, the new calibrated model usually enlarges latent heat flux and raises simulated temperature. Therefore, it reduces simulated temperature biases when its biases are negative but enlarges simulated temperature biases when biases are positive. That is to say that the seasons, weather conditions, and time of day could significantly affect lake model performance because the lake–atmosphere energy flux exchanges may be diverse under different thermal and dynamic contrasts between lake and air (Heikinheimo et al., 1999; Xiao et al., 2013). Thus, it may be more meaningful to establish dynamic parameters based on different weather conditions and lakes.

In addition, the existence of the frontal system for case 3 (06P), precipitation over the region south of 27°N for case 7 (01N), and the precipitation near Lake Poyang and Lake Dongting may result in differences appearing among the results of different cases, such as temperature results for case 2 (02N) and case 7 (01N) and the dew-point temperature for case 7 (07P) and case 8 (07N). What is more, temperature and dew-point temperature near Lake Dongting are more sensitive to the lake–atmosphere coupled model, which may be because Lake Dongting is relatively shallower than Lake Poyang (Venäläinen et al., 1999; Gu et al., 2015).

6. Conclusions

To evaluate the atmosphere–lake coupled model's performance in the Lake Poyang and Lake Dongting regions, we chose eight cases with different weather conditions and conducted three experiments (without the atmosphere–lake coupled model, with the default atmosphere–lake coupled model, and with a new calibrated atmosphere-lake coupled model) for each case. The results show that weather conditions significantly affect lake model performance. That may because of varying water–atmosphere energy flux exchanges under different water–air temperature difference and wind speed conditions (Heikinheimo et al., 1999; Xiao et al., 2013). For the winter with precipitation cases (02P and 01P), the default coupled lake model performs even worse than the experiment without the atmosphere–lake coupled model, and the new calibrated model can reduce 2-m temperature and dew-point temperature biases obviously. For the winter without precipitation cases (02N and 01N), the performance of the experiments without the atmosphere–lake coupled model and with the default model for 2-m temperature show nearly no difference over the Lake Poyang region and at stations far from the lakes, but the experiment without an atmosphere–lake coupled model performs better than the one with the default for 2-m dew-point temperature. The new calibrated model performs best for 2-m temperature over the Lake Poyang region and for 2-m dew-point temperature for all stations, especially over the Lake Dongting region.

For the summer with precipitation case (06P), the experiment without the atmosphere–lake coupled model performs slightly better than that with the default atmosphere–lake coupled model, and the experiment with the new calibrated model performs best over the Lake Poyang region and at stations far from the lakes for 2-m temperature. However, it is difficult to draw a conclusion about which experiment performs better for 2-m dew-point temperature. For the summer with precipitation case (07P) and without precipitation cases (08N and 07N), the three experiments show no clearly obvious differences over the Lake Poyang region and at stations far from the lakes for 2-m temperature. Over the Lake Dongting region, the default and new coupled lake model both significantly reduce 2-m temperature and dew-point temperature biases compared to the experiment without the atmosphere–lake coupled model. The new calibrated model performs best for precipitation and adopting it would reduce simulated precipitation biases of precipitation, especially for the summer with precipitation cases.

Comparatively, temperature and dew-point temperature near Lake Dongting are more sensitive to the lake–atmosphere coupled model. This may be because Lake Dongting is relatively shallower than Lake Poyang (Venäläinen et al., 1999; Gu et al., 2015). Additionally, summer precipitation in the Yangtze River delta and southern China is much higher than winter precipitation and summer precipitation is usually caused by local convection systems, whereas winter precipitation in winter typically due to large-scale circulation; thus, precipitation is more sensitive to the lake–atmosphere coupled model for summer cases than winter cases. Although case 7 (07P) and case 3 (06P) both are summer with precipitation cases, case 3 is affected by a frontal system and the three-day cumulative precipitation for case 3 is much larger than for case 7. Additionally, the weather conditions of case 7 appear to be more like those of case 4 and case 8 (08N and 07N), even though it is a precipitation case. Thus, the performances of the three experiments for case 7 (07P) seem to be similar to those for case 4 and case 8 (08N and 07N). In addition, the WRF model's poor performance with unrealistic simulation of 2-m temperatures for precipitation cases likely attributes to deficiencies in model structure, such as the radiation parameterization scheme, and this cannot be solved completely by improving the lake model, although calibrat-

ing parameters may work.

To sum up, the default coupled lake model performs worse than the experiment without the lake model, and the new calibrated lake model performs best for all stations for winter with precipitation cases. But for other cases, the performance of the default and new calibrated coupled model is complex and the advantage of the new calibrated lake model for 2-m dew-point temperature is greater than that for 2-m temperature. However, for all that, a long-term simulation of five months shows that the new calibrated model still performs better than the default model in the Lake Poyang and Lake Dongting regions.

In fact, the transfer coefficients of momentum, water vapor, and sensible heat flux vary with wind speed and stability conditions (Heikinheimo et al., 1999; Xiao et al., 2013), and the eddy diffusion coefficient should be set differently in dry and wet seasons (Xu et al., 2016; Zhao and Liu, 2017), in shallow and deep lakes (Venäläinen et al., 1999; Gu et al., 2015), and in large and small lakes (Venäläinen et al., 1999). Additionally, water clarity can also affect a lake's light extinction coefficient (Gu et al., 2016). Therefore, we presume that the default and new calibrated model's non-uniform ability to capture 2-m temperature and dew-point temperature and precipitation more realistically is reasonable. Fortunately, the new calibrated model performs better than the default model overall and for a long-term simulation. Based on our analyses, we can draw out that the new model may be more suitable for inclusion in lake-influenced weather and climate studies and may be more meaningful for establishing dynamic parameters based on different weather conditions and lake characteristics.

Acknowledgments. We thank the ECMWF for providing the 6-hourly ERA-Interim dataset (https://rda.ucar.edu/datasets/ds627.0/) as the initial and boundary conditions to drive the WRF model. Besides, we also thank the National Meteorological Information Center of China (http://data.cma.cn) for providing the precipitation, relative humidity, temperature, and dew-point temperature observations data.

REFERENCES

Balsamo, G., R. Salgado, E. Dutra, et al., 2012: On the contribution of lakes in predicting near-surface temperature in a global weather forecasting model. *Tellus A*, **64**, 15829, doi: 10.3402/tellusa.v64i0.15829.

Bullock, O. R. Jr., K. Alapaty, J. A. Herwehe, et al., 2014: An observation-based investigation of nudging in WRF for downscaling surface climate information to 12-km grid spacing. *J. Appl. Meteor. Climatol.*, **53**, 20–33, doi: 10.1175/JAMC-D-13-030.1.

Deng, B., S. D. Liu, W. Xiao, et al., 2013: Evaluation of the CLM4 lake model at a large and shallow freshwater lake. *J. Hydrometeorol.*, **14**, 636–649, doi: 10.1175/JHM-D-12-067.1.

Dutra, E., V. M. Stepanenko, G. Balsamo, et al., 2010: An offline study of the impact of lakes on the performance of the ECMWF surface scheme. *Boreal Environ. Res.*, **15**, 100–112.

Fu, M. N., 2013: Research on the impacts of Poyang Lake on typical weather process and the characteristics of near surface boundary layer. Ph. D. dissertation, Nanjing University of Information Science & Technology, 100 pp. (in Chinese)

Gao, Y., J. S. Fu, J. B. Drake, et al., 2012: Projected changes of extreme weather events in the eastern United States based on a high resolution climate modeling system. *Environ. Res. Lett.*, **7**, 044025, doi: 10.1088/1748-9326/7/4/044025.

Gu, H. P., X. S. Shen, J. M. Jin, et al., 2014: An application of a 1-D thermal diffusion lake model to Lake Taihu. *Acta Meteor. Sinica*, **71**, 719–730, doi: 10.11676/qxxb2013.051.

Gu, H. P., J. M. Jin, Y. H. Wu, et al., 2015: Calibration and validation of lake surface temperature simulations with the coupled WRF-lake model. *Climatic Change*, **129**, 471–483, doi: 10.1007/s10584-013-0978-y.

Gu, H. P., Z. G. Ma, and M. X. Li, 2016: Effect of a large and very shallow lake on local summer precipitation over the Lake Taihu basin in China. *J. Geophys. Res. Atmos.*, **121**, 8832–8848, doi: 10.1002/2015JD024098.

Gula, J., and W. R. Peltier, 2012: Dynamical downscaling over the Great Lakes basin of North America using the WRF regional climate model: The impact of the great lakes system on regional greenhouse warming. *J. Climate*, **25**, 7723–7742, doi: 10.1175/JCLI-D-11-00388.1.

Heikinheimo, M., M. Kangas, T. Tourula, et al., 1999: Momentum and heat fluxes over lakes Tämnaren and Råksjö determined by the bulk-aerodynamic and eddy-correlation methods. *Agric. For. Meteor.*, **98-99**, 521–534, doi: 10.1016/S0168-1923(99)00121-5.

Henderson-Sellers, B., 1986: Calculating the surface energy balance for lake and reservoir modeling: A review. *Rev. Geophys.*, **24**, 625–649, doi: 10.1029/RG024i003p00625.

Hong, S. Y., and J. O. J. Lim, 2006: The WRF single-moment 6-class microphysics scheme (WSM6). *J. Korean Meteor. Soc.*, **42**, 129–151.

Hostetler, S. W., and P. J. Bartlein, 1990: Simulation of lake evaporation with application to modeling lake level variations of Harney–Malheur Lake, Oregon. *Water Resour. Res.*, **26**, 2603–2612, doi: 10.1029/WR026i010p02603.

Hostetler, S. W., G. T. Bates, and F. Giorgi, 1993: Interactive coupling of a lake thermal model with a regional climate model. *J. Geophys. Res. Atmos.*, **98**, 5045–5057, doi: 10.1029/92JD02843.

Hostetler, S. W., F. Giorgi, G. T. Bates, et al., 1994: Lake–atmosphere feedbacks associated with paleolakes Bonneville and Lahontan. *Science*, **263**, 665–668, doi: 10.1126/science.263.5147.665.

Kain, J. S., 2004: The Kain–Fritsch convective parameterization: An update. *J. Appl. Meteor.*, **43**, 170–181, doi: 10.1175/1520-0450(2004)043<0170:TKCPAU>2.0.CO;2.

Klaić, Z. B., and M. Kvakić, 2014: Modeling the impacts of a man-made lake on the meteorological conditions of the sur-

rounding areas. *J. Appl. Meteor. Climatol.*, **53**, 1121–1142, doi: 10.1175/JAMC-D-13-0163.1.

Li, R., J. Jin, S. Y. Wang, et al., 2014: Significant impacts of radiation physics in the Weather Research and Forecasting model on the precipitation and dynamics of the West African Monsoon. *Climate Dyn.*, **44**, 1583–1594, doi: 10.1007/s00382-014-2294-2.

Lin, B. Y., and M. X. Li, 1988: Characteristic feature of the lake-land breeze and its effect on precipitation over the Dongtinghu Lake. *J. Nanjing Inst. Meteor.*, **11**, 78–88. (in Chinese)

Lofgren, B. M., 1997: Simulated effects of idealized Laurentian Great Lakes on regional and large-scale climate. *J. Climate*, **10**, 2847–2858, doi: 10.1175/1520-0442(1997)010<2847:SEOILG>2.0.CO;2.

Long, Z., W. Perrie, J. Gyakum, et al., 2007: Northern lake impacts on local seasonal climate. *J. Hydrometeorol.*, **8**, 881–896, doi: 10.1175/JHM591.1.

Mallard, M. S., C. G. Nolte, O. R. Bullock, et al., 2014: Using a coupled lake model with WRF for dynamical downscaling. *J. Geophys. Res. Atmos.*, **119**, 7193–7208, doi: 10.1002/2014JD021785.

Mallard, M. S., C. G. Nolte, T. L. Spero, et al., 2015: Technical challenges and solutions in representing lakes when using WRF in downscaling applications. *Geosci. Model Dev.*, **8**, 1085–1096, doi: 10.5194/gmd-8-1085-2015.

Martynov, A., L. Sushama, R. Laprise, et al., 2016: Interactive lakes in the Canadian Regional Climate Model, version 5: The role of lakes in the regional climate of North America. *Tellus A*, **68**, 16226, doi: 10.3402/tellusa.v64i0.16226 .

Meng, X. H., Evans, J. P., and M. F. McCabe, 2014: The impact of observed vegetation changes on land–atmosphere feedbacks during drought. *J. Hydrometeorol.*, **15**, 759–776, doi: 10.1175/JHM-D-13-0130.1.

Meng, X. H., S. H. Lyu, T. T. Zhang, et al., 2018: Simulated cold bias being improved by using MODIS time-varying albedo in the Tibetan Plateau in WRF model. *Environ. Res. Lett.*, **13**, 044028, doi: 10.1088/1748-9326/aab44a.

Mlawer, E. J., S. J. Taubman, P. D. Brown, et al., 1997: Radiative transfer for inhomogeneous atmospheres: RRTM, a validated correlated-k model for the longwave. *J. Geophys. Res. Atmos.*, **102**, 16663–16682, doi: 10.1029/97JD00237.

Niu, G. Y., Z. L. Yang, K. E. Mitchell, et al., 2011: The community Noah land surface model with multiparameterization options (Noah-MP): 1. Model description and evaluation with local-scale measurements. *J. Geophys. Res. Atmos.*, **116**, D12109, doi: 10.1029/2010JD015139.

Noh, Y., W. Cheon, S. Y. Hong, et al., 2003: Improvement of the K-profile model for the planetary boundary layer based on large eddy simulation data. *Bound.-Layer Meteor.*, **107**, 401–427, doi: 10.1023/A:1022146015946.

Notaro, M., K. Holman, A. Zarrin, et al., 2013: Influence of the Laurentian Great Lakes on regional climate. *J. Climate*, **26**, 789–804, doi: 10.1175/JCLI-D-12-00140.1.

Oleson, K. W., D. M. Lawrence, G. B. Bonan, et al., 2013: Technical Description of Version 4.5 of the Community Land Model (CLM). NCAR Technical Note NCAR/TN-503+STR, Boulder, Colorado: NCAR Earth System Laboratory, doi: 10.5065/D6RR1W7M

Samuelsson, P., E. Kourzeneva, and D. Mironov, 2010: The impact of lakes on the European climate as simulated by a regional climate model. *Boreal Environ. Res.*, **15**, 113–129.

Schmidlin, T. W., 2005. *Lakes, Effects on Climate*. Springer, Dordrecht, 444–445, doi: 10.1007/1-4020-3266-8_119.

Scott, R. W., and F. A. Huff, 1996: Impacts of the Great Lakes on regional climate conditions. *J. Great Lakes Res.*, **22**, 845–863, doi: 10.1016/S0380-1330(96)71006-7.

Scott, R. W., and F. A. Huff, 1997: Lake Effects on Climatic Conditions in the Great Lakes Basin. ISWS Contract Report CR-617, Illinois State Water Survey, Illinois, 73 pp.

Sills, D. M. L., J. R. Brook, I. Levy, et al., 2011: Lake breezes in the southern Great Lakes region and their influence during BAQS-Met 2007. *Atmos. Chem. Phys.*, **11**, 7955–7973, doi: 10.5194/acp-11-7955-2011.

Stepanenko, V. M., A. Martynov, K. D. Jöhnk, et al., 2013: A one-dimensional model intercomparison study of thermal regime of a shallow, turbid midlatitude lake. *Geosci. Model Dev.*, **6**, 1337–1352, doi: 10.5194/gmd-6-1337-2013.

Subin, Z. M., W. J. Riley, and D. Mironov, 2012: An improved lake model for climate simulations: Model structure, evaluation, and sensitivity analyses in CESM1. *J. Adv. Mod. Earth Syst.*, **4**, M02001, doi: 10.1029/2011MS000072.

Venäläinen, A., M. Frech, M. Heikinheimo, et al., 1999: Comparison of latent and sensible heat fluxes over boreal lakes with concurrent fluxes over a forest: Implications for regional averaging. *Agric. For. Meteor.*, **98–99**, 535–546, doi: 10.1016/S0168-1923(99)00100-8.

Wang, X. F., and Z. J. Liu, 2008: Statistical characteristics of tropical cyclones making landfalls and passing through lakes in China. *J. Trop. Meteor.*, **24**, 539–545, doi: 10.3969/j.issn.1004-4965.2008.05.015. (in Chinese)

Xiao, W., S. D. Liu, W. Wang, et al., 2013: Transfer coefficients of momentum, heat and water vapour in the atmospheric surface layer of a large freshwater lake. *Bound.-Layer Meteor.*, **148**, 479–494, doi: 10.1007/s10546-013-9827-9.

Xu, L. J., H. Z. Liu, Q. Du, et al., 2016: Evaluation of the WRF-lake model over a highland freshwater lake in Southwest China. *J. Geophys. Res. Atmos.*, **121**, 13989–14005, doi: 10.1002/2016JD025396.

Zhao, X. S., and Y. B. Liu, 2017: Phase transition of surface energy exchange in China's largest freshwater lake. *Agric. For. Meteor.*, **244–245**, 98–110, doi: 10.1016/j.agrformet.2017.05.024.

Tech & Copy Editor: Zhirong CHEN